Klyatskina, E.; Segovia-López, F.; Salvador Moya, MD.; Sanchez, E.; Stolyarov, V. (2022). Mechanical Behavior Monitored by Acoustic Emission of Nanostructured Alumina-Titania Coatings. Journal of Machinery Manufacture and Reliability. 51(5):441-446. https://doi.org/10.3103/S1052618822050065

УДК [539.23]1, P.A.C.S. [62.20:68]

MECHANICAL BEHAVIOR MONITORED BY ACOUSTIC EMISSION OF NANOSTRUCTURED ALUMINA-TITANIA COATINGS

E. Klyatskina [†1], F. Segovia[1], M. D. Salvador[1], E. Sanchez[2]; V.V. Stolyarov[3]

[1]*Instituto de Tecnología de Materiales. ITM, Universitat Politècnica de Valéncia, Valencia, Spain*

[2]*Instituto de Tecnología Cerámica. ITC, Universitat Jaume I. Castellón, Spain*

[3]*Mechanical Engineering Research Institute of Russian Academia of Sciences, Moscow, Russia*

[†]*e-mail: elkl1@upvnet.upv.es*

This study aims to evaluate the mechanical behavior of nanostructured and conventional alumina-titania coatings by means of combining four-point bend tests monitored with acoustic emission. Determination of bending strength, along with information received from acoustic emission signal, such as quantity, amplitude, energy and length of events gives a better understanding of failure mechanisms in coatings. This information has been complemented with optical analysis of fracture surfaces. Failure of coatings has been observed to follow four stages that are clearly defined in the acoustic emission data. This fracture behavior has been observed for all three types of coating tested, but the nanostructured coating presented the best combination of hardness and strength, due to its duplex microstructure.

Keywords: *atmospheric plasma spraying, nanostructured coatings, alumina-titania acoustic emission, four-point bend test.*

1. Introduction

To present, one of the main ways of industrial development is to increase reliability of existing technical machinery, to reduce maintenance cost and to extend its lifespan so as to ensure its competitiveness in the marketplace. The use of surface protection technologies is a key line in resolving these technological issues [1].

Atmospheric plasma spray (APS) is the most widely used spraying technique in industrial applications in order to obtain ceramic coatings due to its versatility and low-cost. Thermal spraying methods that produce alumina-titania coatings are optimal technologies for improving wear and corrosion resistance on the surface of the substrates in a variety of key industrial applications such as aerospace, automobile, energy, cutting tools, as well as petroleum. The coatings are heat resistant to about 540°C, are resistant to most acids and alkalies, and have high dielectric strength. Aluminum Titania coatings are commonly used in the chemical and textile industries where smooth and dense deposits with high friction resistance is required. The coating has been used successfully in motor housings, electric railways, and electric components. It's high service temperatures have made it a good candidate for rocket engine thrust chambers and jet engines [2, 3].

One of the greatest limitations of ceramic materials is their inherent brittleness. In fact, ceramic coatings usually fail by cracking, detachment or delamination instead of being degraded by wear during service [4]. Furthermore, a coating produced by plasma spraying presents a very varied microstructure. Microhardness measurements have been used to typify coatings. However, hardness does not always show a good correlation with other mechanical properties of the coatings [2]. Due to these limitations, a specific standardized test is needed to evaluate mechanical properties of the coatings [4]. Macro and micro fractures, amongst other sources, may release energy during the coating service and therefore these can be detected by means of acoustic emission giving a better and more detailed understanding of failure mechanisms in coatings. This is the principle in which this study is based.

A combined method employing both mechanical testing and in-situ acoustic emission is a powerful tool to analyze the failure mechanism of coating obtained by thermal spraying. The acoustic emission method is very sensitive to the type of defects including size and number of defects, adhesive and/or cohesive force, and their orientation with regard to stress applied [5, 6]. The differences in microstructure induced by plasma deposition process may have significant effects on bending strength and therefore the application of acoustic emission techniques may explain the fracture mechanisms associated with those differences.

In the present study the use of four-point bending testing combined with acoustic emission analysis have been carried out in three different alumina-titania coatings processed by APS in order to elucidate the fracture mechanisms involved and to evaluate the mechanical behavior.

2. Methodology

Three types of commercial alumina-titania powders were used in this study: conventional micrometric powder (Sulzer Metco 130, particle size 30 - 50 μm), nano-sized powder (Infranat S2613S, particle size 20 - 60 nm) and densified nanostructured powder (Inframat S2613P) with agglomerates of micrometric size between 15 and 40 μm. All powders have the same chemical and stoichiometric composition: 87 wt.%Al_2O_3 and 13wt.% TiO_2.

A Sulzer MetcoTM atmospheric plasma torch fitted with F4-MB nozzle was used to plasma spray the powders. The deposition parameters provided by the powder suppliers have been slightly modified to obtain optimum characteristics for each coating [7].

Six specimens were tested for each of sample. All the ceramic coatings were deposited up to a thickness of 100-150 μm on stainless steel sheets AISI 316L grade about 2 mm thick. Steel substrate samples were pre-cleaned and fine grit blasted to a roughness of 1.69 μm. The influence of bonding coating on the adhesion of the ceramic was also analyzed. For this, one series of samples were coated by plasma spraying with a nickel-based alloy AMDRY 995C (composition Co32Ni21Cr8Al0.5Y) to from a bonding layer about 45 ± 5 μm thick. In order to further optimize

the adherence of the coatings preheating of the substrate was carried out before spraying. The temperature of the substrate during the process was kept at about 150 ± 50 ºC [7]. An Instron 4202 universal testing machine was used to perform the four-point bending test at a crosshead speed of 0.5 mm/min. A four-point bend test was chosen because it assures a constant stress between the two central supports. This test is accepted by several sources [8, 9] because it enables to test the coating under tensile stress and the substrate under compression. Samples were placed with the coating facing down on the supports. Specimen dimensions were 49 ± 1 mm long and 8.0 ± 0.5 mm wide. The outer span/sample thickness ratio was 16:1, whereas the outer/inner span ratio was 1:2. The test is ended when delamination of the coating is observed. Stresses σ (MPa) in the coating are calculated following the expression (1),

$$\sigma = \frac{3 \cdot F \cdot L}{4 \cdot b \cdot h^2} \qquad (1)$$

where F is force applied (N), L is span length (mm), b is width (mm) and h is specimen thickness (mm).

The methodology for determining the characteristic stresses was described in an earlier published work and included a series of experiments with different loads and the determination of the number of cracks on the sample using an optical microscope [9]. Acoustic emission sensors were place symmetrically on the support base of the bending tool. This choice is conditioned by the smaller thickness of the sample and configuration of the test device, sensors size and fixation grips. The acoustic emission recording was performed simultaneously to the bending test. The equipment was a Vallen AMSY-5 acoustic emission apparatus, with AEP4 type sensors working at 150 kHz resonance frequency with 34 dB preamplification.

The threshold amplitude was set to 40 dB. This noise level was determined during the testing of uncoated steel. Thus, any background noise arising from the mechanical test device was filtered and removed from analysis. An acoustic emission (AE) event is detected, amplified and studied in terms of amplitude, absolute energy and number of hits. Absolute energy is a software calculated parameter which corresponds to the real energy produced during the AE event. One hit corresponds

to the detection of one burst signal on a channel. One event can include several hits. Furthermore, and in order to discriminate the different stages of material fracture, intermediate microstructural examinations were carried out during the tests.

3. Results and discussion

Microstructure and phase composition of these coatings have been described in previous works [7]. The micrometric coating presents a laminar microstructure of flattened layers or "splats" of solid solution of titania and alumina in variable composition. This coating equally presents microcracks in the direction perpendicular to the layers, produced by thermal stresses and interlaminar porosity. On the other hand, the nanometric coating presents a "duplex" structure consisting in partially fused particles of the initial powder located between crushed layers; this is the result of the size of the starting particles forming porous agglomerates difficult to melt by their own nature. The commercial densified nanostructured coating has a similar microstructure to that of nanometric powder, but is differentiated by the size of the partially fused particles.

The loading curve and acoustic emission records for a coating specimen from densified nanostructured powder are presented in fig. 1.

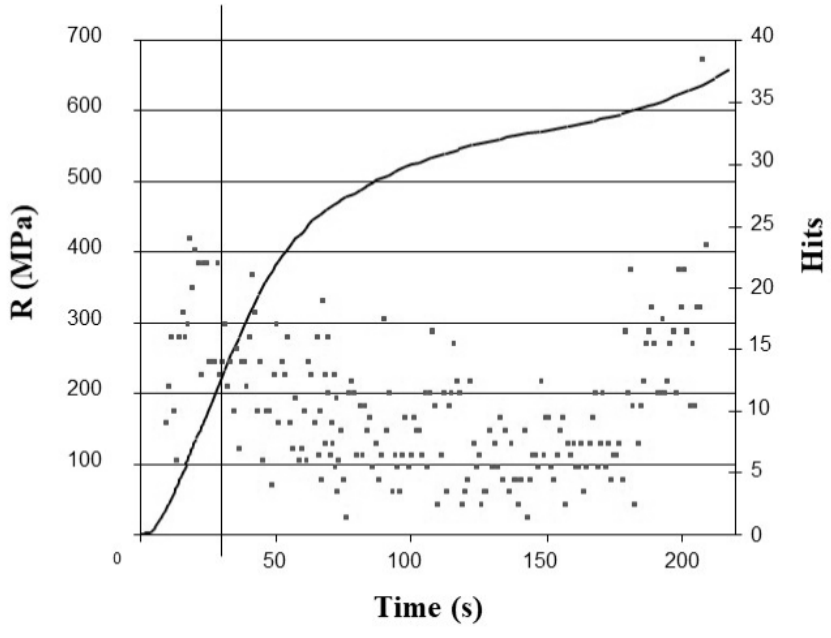

a

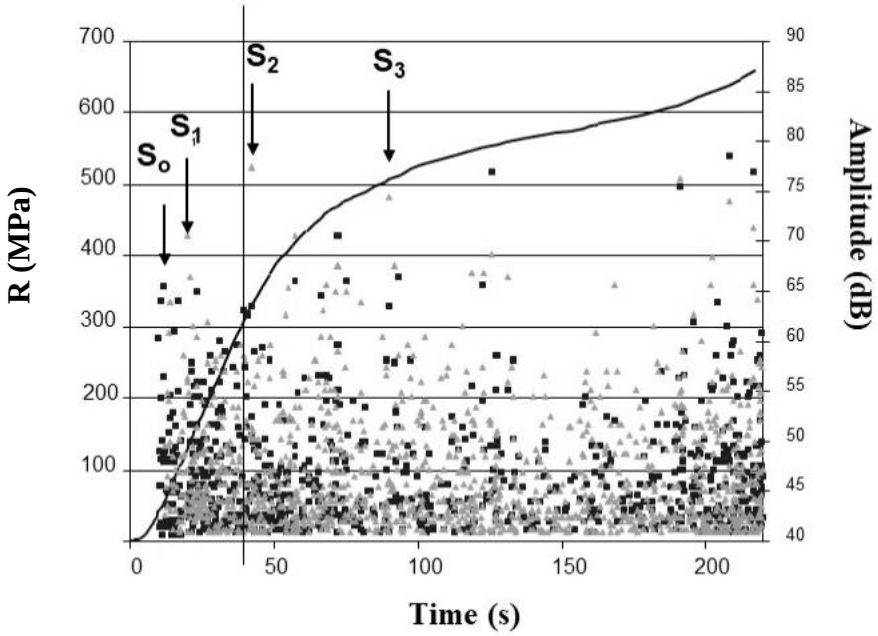

b

Fig. 1. Stress bending curve and acoustic emission registers for specimen with bond coating: (a) hits, (b) amplitude of events.

The bending stress-displacement curves have been replaced by stress-time curves in order to clarify the relation between mechanical and acoustic behaviour. Stress-time curves present the classic elastoplastic behaviour for loading curve obtained from bending tests. During the test the occurrence of a hit with amplitude higher than the threshold level, set at 40 dB, denotes that some kind of event has happened in the coating as an effect of the applied stress.

The failure mechanism of metal-ceramic coatings proposed by authors [11-13] take place in 3 stages: (1) formation of microcracks, (2) propagation, and (3) collapse through delamination. These works provide a relationship between acoustic emission data and bending stresses to identify these stages in the deterioration mechanism. Failure stresses of all coating shown in the table 1.

Table 1. Failure stresses of coatings.

Stress (MPa)	Micrometric	Nanometric	Nanostructured
Without bond layer			
S_0	15 ± 3	18 ± 3	28 ± 7
S_1	36 ± 7	62 ± 6	68 ± 3
S_2	62 ± 3	184 ± 6	172 ± 5
S_3	228 ± 21	216 ± 5	287 ± 17
With bond layer			
S_0	27 ± 4	20 ± 6	41 ± 8
S_1	58 ± 8	73 ± 4	121 ± 9
S_2	175 ± 21	220 ± 14	362 ± 45
S_3	271 ± 13	404 ± 37	475 ± 25

At the beginning of the test the first acoustic activity appears at very low stresses, fig. 1 (a). The amplitude of those AE events is lesser than 55 dB, fig. 1 (b). For that level of stress, the formation of microcracks occurs in the zones affected by thermal stresses during processing. S_0 represents the stress associated to occurrence of the first event, fig. 1 (a). These results confirm those obtained by [11] in similar alumina-titania coatings, relative to the amplitude of events in the first degradation stage. However, due to the intrinsic brittle behaviour of the coatings studied in the present work, the stress level S_0 related to the first stage is lower than that found in metal-ceramic coating [14].

The propagation and coalescence of microcracks are found in the ceramic coating to take place during the linear response of the material, corresponding to transition period from elastic to plastic behaviour of substrate. The AE spectrum shows increasing activity during this period. During this stage the stress S_1 is defined by the occurrence of an event of maximum amplitude in the range from 40 dB to 70 dB, fig. 1 (b).

Fig. 2 represents (a) the distribution of hits as a function of energy in attojoules aJ (10^{-18} J) and (b) the relationship between energy and amplitude (dB), for coated specimen with bond coating from nanostructured densified powder.

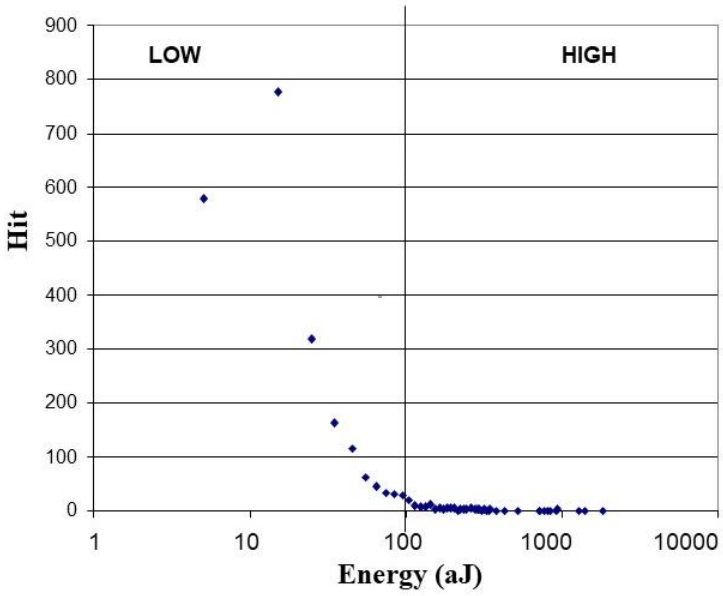

a

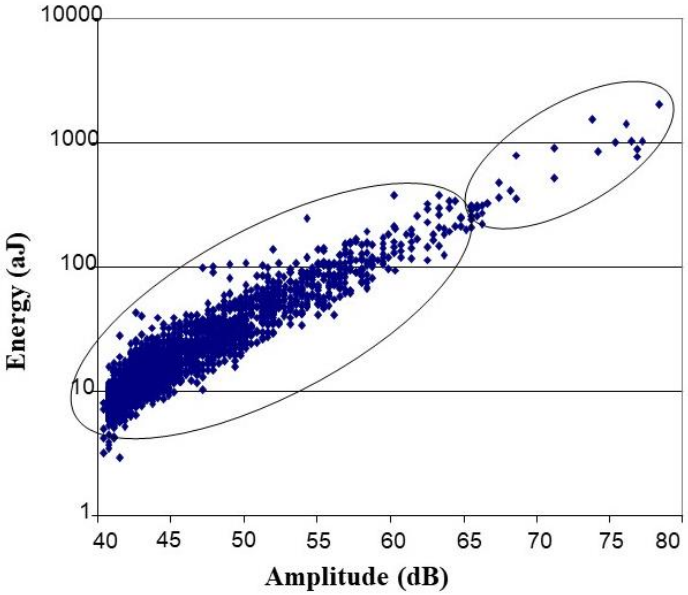

b

Fig. 2. Acoustic emission results of bending test (a) number of hits as a function of their energy and (b) energy as a function of the amplitude.

Analysis of these results shows that the majority of events detected during this period are characterized by presenting a low energy comprised between 1 and 100 aJ, fig. 2 (a). This population events of low energy and amplitude are located on the left of fig. 2 (b).

AE events with maximum amplitude are observed in the plastic part of the loading curve. At this moment the first transversal macro crack was observed. For that reason, the stress S_2 is defined in figure 1 (b) to the appearance of events with amplitude upper 70 dB. At higher stresses than S_2 a network of microcracks starts to form, in agreement with [12]. Subsequent events over 70 dB are also associated to the formation of new networks or the growth of the existing ones.

The characteristic stress S_3 corresponds to the catastrophic failure, including delamination and detachment of coating, which was found in the non-linear field corresponding to high bending load. It is characterised by the appearance of strong amplitude AE events above 75 dB which is the evidence of severe damage of the coating. These values of characteristic stress are presented in table 1.

After complete load test AE results indicate that only the events characterized by high energy, around 1000 aJ, and high amplitude (fig. 2 (b)) are related to the apparition of transversal macrocraks and delamination. These events with high energy level and amplitude are located in upper right area of fig. 2 (b). These values are consistent with those found for similar coatings [13].

First of all, it should be pointed that all characteristic stresses S are greater for the coatings with bonding layer than for those without. Visual observation of the samples without bonding layer reveals a single catastrophic crack which gives rise to subsequent delamination, for instance, as in the case of the nanometric coating at 216 MPa. In fact, apparent cracks are not observed on the coating with bonding layer tested to the same stress. This fact proves the importance of the bonding layer for improving coating adherence. The catastrophic crack for the nanometric coating with bonding layer appears visible at higher load level, 404 MPa.

Multiple transversal cracking along the whole coating surface is present after this stress level is reached. This behaviour could be extended to the rest of coatings studied (micrometric and nanostructured densified). These results are explained by the hypothesis the bonding layer enables those stresses to be distributed more uniformly ensuring greater adherence to the substrate.

Concerning type of coating, there are also differences in the characteristic stresses, table 1. The samples with nanostructured densified coating give the highest values from S_0 to S_3, whereas for micrometric and nanometric coating these values are lower. On the other hand, when considering also the presence of bonding layer, the final collapse of the micrometric coatings occurred at lower stress levels than the nanometric and densified nanostructured coatings. This result is due to differences in the crack propagation mechanism as explained by [11, 15].

The fracture cracks in conventional micrometric coatings propagate following splat limits which mark the edges between each deposited droplet. In nanostructured coatings, cracks do not follow splat limits. They propagate through the nanostructured particles until they reach a region of longer grains, formed from the partially melted feeder material. Any stress applied on the nanostructured coating is compensated by the formation of transversal microcracks that are stopped before they can propagate further to link up with other cracks. For this reason, the number of AE hits is much lower for the micrometric coating in comparison to the registers of both nanometric and densified coatings, regardless of the presence of bonding layer.

Microhardness of the micrometric coatings is HV_{200}=850 ± 110, the nanometric is HV_{200}=780 ± 80 and the nanostructured is HV_{200}=845 ± 90. Comparing characteristic stresses with hardness for the different coatings, there is not an evident relationship. In fact, although micrometric coating exhibits the highest hardness value characteristic stresses remain lower. This is indicative that fracture mechanism related to phases and splats boundary microstructure which plays an important role in the behaviour of the materials. In fact, the presence of phases in the nanometric ranges provides higher bond strength, resulting in higher characteristic stresses, which points to a better toughness behaviour. When comparing both nanocoatings, mechanical strength is much better for nanostructured (densified) material as a result of its lower porosity and higher hardness for similar fracture behaviour.

4. Summary

Plasma spray coatings from different feedstocks - micrometric, nanometric and densified nanostructured- have been analysed by bending tests monitored with acoustic emission and correlated to microstructural features, in order to better understand the mechanism of fracture. The main conclusions drawn are the following:

- The mechanism of fracture of coatings comprises four stages: generation of microcracks in the zone with high concentration of thermal stresses between the splashed layers, microcracks propagation and coalescence, formation of a first transversal macro crack and finally catastrophic failure in the form of delamination and detachment of the coating.

- In the case of micrometric coatings, the characteristic stresses for the four-damage mechanism are lower than those of the nanostructured coatings. The final collapse of the coating occurs with a less stress.

- In all cases the presence of the bonding layer improves the adherence of the coating to the substrate. Accordingly, the characteristic stresses of the four-damage mechanism are higher for coatings with bonding layer.

- The nanostructured coating presents the best combination of hardness and strength, because of its duplex microstructure that provide the toughness behaviour against the crack propagation.

Conflict of interests. The authors declare that they have no conflict of interest.

REFERENCES:

1. Luo L., Chen Y., Zhou M., Shan X., Lu J., Zhao X., Progress update on extending the durability of air plasma sprayed thermal barrier coatings, Ceram. Inter. 2022, 48, (13), p. 8021-18034, DOI:10.1016/j.ceramint.2022.04.044.
2. P.G. Lashmi, P.V. Ananthapadmanabhan, G. Unnikrishnan, S.T. Aruna, Present status and future prospects of plasma sprayed multilayered thermal barrier coating systems, J. Eur. Ceram. Soc., 2020, 40 (8), p. 2731-2745, DOI:10.1016/j.jeurceramsoc.2020.03.016.
3. Fathi R., Wei H., Saleh B., Radhika N., Jiang J., Ma A., Ahmed M. , Li Ostrikov K., Past and present of functionally graded coatings: Advancements and future challenges, Appl. Mater. Today 2022, 25, p.101373
4. Wu X.J., The crack number density theory on air-plasma-sprayed thermal barrier coating, Surf. Coat. Technol. 2019, 358, p. 347-352, DOI:10.1016/j.surfcoat.2018.11.058.
5. Wang L., Ming C., Zhong X.H., Ni J.X., Tao S.Y., F.F. Zhou, Wang Y., Prediction of critical rupture of plasma-sprayed yttria stabilized zirconia thermal barrier coatings under burner rig test via finite element simulation and in-situ acoustic emission technique, Surf. Coat. Technol. 2019, 367, 58-74, DOI:10.1016/j.surfcoat.2019.03.063.
6. Yao W.B., Dai C.Y., Mao W.G., Lu C., Yang L., Zhou Y.C., Acoustic emission analysis on tensile failure of air plasma-sprayed thermal barrier coatings, Surf. Coat. Technol. 2012, 206,18, 3803-3807, DOI:10.1016/j.surfcoat.2012.03.050.
7. Sánchez E., Moreno A., Vicent M., Salvador M.D., Bonache V., Klyatskina E., Santacruz I., Moreno R., Preparation and spray drying of Al2O3–TiO2 nanoparticle suspensions to obtain nanostructured coatings by APS. J. Surf. Coat. Technol. 205 (4), 987 (2010) DOI:10.1016/j.surfcoat.2010.06.002.
8. Cox L.C., The four-point bend test as a tool for coating characterization. J. Surf. Coat. Technol. 1988, 36 (3), 807 DOI:10.1016/0257-8972(88)90021-7.

9. Richard C.S., Beranger G., Lu J., Flavenot J.F., Gregoire T., Four-point bending tests of thermally produced WC-Co coatings. Surf. Coat. Technol. 1996, 78 (1), 284, doi.org/10.1016/0257-8972(95)02416-6.
10. Segovia F., Klyatskina E., Bonache V., Salvador Mª.D., Sanchez E., Cantavella V., Bloem C., Acoustic emission study on flexural behaviour of WC-Co coatings obtained by atmospheric plasma spray. Rev. Metal. CENIM 2007, 43 (6), 414, DOI: 10.3989/revmetalm.2007.v43.i6.84.
11. Bansal P., Padture N.P., Vasiliev A., Improved interfacial mechanical properties of Al2O3-13wt%TiO2 plasma-sprayed coatings derived from nanocrystalline powders. Acta Mater. 2003, 51, 2959, DOI: 10.1016/s1359-6454(03)00109-5.
12. Dalmas D., Benmedakhene S., Richard C., Laksimi A., Béranger G., Grégoire T., Caractérisation par émission acoustique de l'adhérence et de l'endommagement d'un revêtement : cas d'un revêtement WC–Co sur acier. Chemistry 2001, 4(5), 345, DOI:10.1016/S1387-1609(01)01240-3.
13. Miguel J.M., Guilemany J.M., Mellor B.G., Xu Y.M., Acoustic emission study on WC–Co thermal sprayed coatings. Mater. Sci. Eng. 2003, 352, 55, DOI:10.1016/S0921-5093(02)00546-4.
14. Sarikaya O., Effect of some parameters on microstructure and hardness of alumina coatings prepared by the air plasma spraying process. Surf. Coat. Technol. 2005, 190 (2–3), p. 388-393, DOI:10.1016/j.surfcoat.2004.02.007.
15. Yılmaz R., Kurt A.O., Demir A., Tatli Z., Effects of TiO2 on the mechanical properties of the Al2O3–TiO2 plasma sprayed coating. J. Eur. Ceram. Soc. 2007, 27, 1319, DOI: 10.1016/j.jeurceramsoc.2006.04.099.